

We are IntechOpen, the world's leading publisher of Open Access books Built by scientists, for scientists

4,800

Open access books available

122,000

International authors and editors

135M

Downloads

Our authors are among the

154

Countries delivered to

TOP 1%

most cited scientists

12.2%

Contributors from top 500 universities



WEB OF SCIENCE™

Selection of our books indexed in the Book Citation Index
in Web of Science™ Core Collection (BKCI)

Interested in publishing with us?
Contact book.department@intechopen.com

Numbers displayed above are based on latest data collected.

For more information visit www.intechopen.com



Robust Feedback Linearization Approach for Fuel-Optimal Oriented Control of Turbocharged Spark-Ignition Engines

Anh-Tu Nguyen, Thierry-Marie Guerra and Jimmy Lauber

Abstract

This chapter proposes a new control approach for the turbocharged air system of a gasoline engine. To simplify the control implementation task, static lookup tables (LUTs) of engine data are used to estimate the engine variables in place of complex dynamical observer and/or estimators. The nonlinear control design is based on the concept of robust feedback linearization which can account for the modeling uncertainty and the estimation errors induced by the use of engine lookup tables. The control feedback gain can be effectively computed from a convex optimization problem. Two control strategies have been investigated for this complex system: drivability optimization and fuel reduction. The effectiveness of the proposed control approach is clearly demonstrated with an advanced engine simulator.

Keywords: turbocharged gasoline engine, engine control, robust control, feedback linearization, linear matrix inequality

1. Introduction

The control of turbocharged air system of spark-ignition (SI) engines is known as a challenging issue in automotive industry. It is complex and costly to develop and implement a new control strategy within industrial context since it may change the available software in series [1]. The novel control strategies, generally needed when some new technologies are introduced, have to justify its relevant advantages with respect to the actual versions. At the same time, they have to satisfy several stringent constraints such as control performance/robustness, calibration complexity, and software consistency. Therefore, conventional control approaches are still largely adopted by automakers. These control strategies consist in combining the gain-scheduling PID control with static feedforward lookup table (LUT) control [2]. This results in an easy-to-implement control scheme for the engine control unit (ECU). However, such a conventional control strategy remains some inherent drawbacks. First, using gain-scheduling PID control technique and static feedforward LUTs, each engine operating point needs to be defined, leading to heavy calibration efforts. In addition, it is not always clear to define an engine operating point, in particular for complex air system with multiple air actuators [1].

Second, the trade-off between performance and robustness is not easy to achieve for a wide operating range of automotive engines. Therefore, conventional control strategies may not be appropriate to cope with new engine generations for which many novel technologies have been introduced to meet more and more stringent legislation constraints. Model-based control approaches seem to be a promising solution to overcome these drawbacks.

Since turbochargers are key components in downsizing and supercharging technology, many works have been recently devoted to the turbocharged engine control. A large number of advanced model-based control techniques have been studied in the literature, e.g., gain-scheduling PID control [3, 4], H_∞ control [5], gain-scheduling H_∞ control [6], sliding mode control [7], predictive control [8], etc. These control techniques are based on engine model linearization to apply linear control theory. Hence, the calibration efforts are expensive and the aforementioned drawbacks still remain. Nonlinear control seems to be more relevant for this complex nonlinear system. Most of the efforts have been devoted to diesel engine control [9–11], and only some few works have focused on SI engine control. In [1], the authors proposed an interesting approach based on flatness property of the system combining feedback linearization and constrained motion planning to meet the predefined closed-loop specifications. However, due to the robustness issue with respect to the modeling uncertainty, this control approach requires a refined control-based engine model to provide a satisfactory control performance. To avoid this drawback, many robust nonlinear control approaches have been proposed for turbocharged engine control, for instance, fuzzy sliding mode control [12], double closed-loop nonlinear control [13], nonlinear model predictive control [14], and so forth. However, for most of the existing control approaches, it is not easy to take into account the *fuel-optimal strategy* [15] in the control design when considering the whole system. To get rid of this difficulty, a novel control strategy based on switching Takagi-Sugeno fuzzy model has been proposed in switching control [16–18]. Although this powerful nonlinear control approach provides satisfactory closed-loop performance, it may look complex from the industrial point of view. In this chapter, we propose a new control design based on feedback linearization for the turbocharged air system which is much simpler (in the sense of real-time implementation) and can achieve practically a similar level of performance as in [19]. To the best of our knowledge, this is the second nonlinear multi-input multi-output (MIMO) control approach that can guarantee the stability of the whole closed-loop turbocharged air system while taking into account the *fuel-optimal strategy* after [20]. Furthermore, the proposed control approach allows reducing the costly automotive sensors and/or observers/estimators design tasks by exploiting the maximum possible available offline information. The idea is to estimate all variables needed for control design by using piecewise multi-affine (PMA) modeling [21, 22], represented in the form of static LUTs issued from the data of the test bench. The effectiveness of the proposed control strategy is illustrated through extensive AMESim/Simulink co-simulations with a high-fidelity AMESim engine model.

The chapter is organized as follows. Section 2 reviews some basis on feedback linearization. In Section 3, a new robust control design based on this technique is proposed in some detail. Section 4 is devoted to the control problem of a turbocharged air system of a SI engine. To this end, a brief description of this system is first recalled. Besides a conventional MIMO control approach, a novel idea is also proposed to take into account the strategy for minimizing the engine pumping losses in the control design. Then, simulation results are presented to show the effectiveness of our proposed method. Finally, some concluding remarks are given in Section 5.

2. Feedback linearization control

Feedback linearization provides a systematic control design procedure for nonlinear systems. The main idea is to algebraically transform nonlinear system dynamics into a (fully or partly) linear one so that the linear control techniques can be applied [23, 24]. However, it is well known that this technique is based on the principle of exact nonlinearity cancelation. Hence, it requires high-fidelity control-based models [25]. This is directly related to the closed-loop robustness property with respect to model uncertainties. To this end, a new robust design dealing with model uncertainties/perturbations will be proposed. Compared to some other existing results on robust feedback linearization [24, 26, 27], the proposed method not only is simple and constructive but also maximizes the robustness bound of the closed-loop system through a linear matrix inequality (LMI) optimization problem [28]. Furthermore, this method may be applied to a large class of nonlinear systems which are input-output linearizable and possess stable internal dynamics.

For engine control purposes, we consider the following input-output linearization for MIMO nonlinear systems:

$$\begin{cases} \dot{x}(t) = f(x) + \sum_{i=1}^m g_i(x)u_i(t) \\ y(t) = h(x) \triangleq [h_1(x), \dots, h_m(x)]^T \end{cases} \quad (1)$$

where $x(t) \in \mathbb{R}^n$ is the system state, $u(t) \in \mathbb{R}^m$ is the control input, and $y(t) \in \mathbb{R}^m$ is the measured output. The matrix functions $f(x)$, $g(x)$, and $h(x)$ are assumed to be sufficiently smooth in a domain $D \subset \mathbb{R}^n$. For simplicity, the time dependence of the variables is omitted when convenient.

The feedback linearization control law of the system (1) is given by

$$u(t) = \begin{bmatrix} L_{g_1} L_f^{\rho_1 - 1} h_1(x) & \dots & L_{g_m} L_f^{\rho_1 - 1} h_1(x) \\ \dots & \dots & \dots \\ L_{g_1} L_f^{\rho_m - 1} h_m(x) & \dots & L_{g_m} L_f^{\rho_m - 1} h_m(x) \end{bmatrix}^{-1} \left(\begin{bmatrix} v_1(t) \\ \vdots \\ v_m(t) \end{bmatrix} - \begin{bmatrix} L_f^{\rho_1} h_1(x) \\ \vdots \\ L_f^{\rho_m} h_m(x) \end{bmatrix} \right) \triangleq J^{-1}(x)(v(t) - l(x)) \quad (2)$$

where $[\rho_1 \dots \rho_m]^T$ is the vector of relative degree and v is a vector of new manipulated inputs. The Lie derivatives $L_f^{\rho_i} h_i(x)$ and $L_{g_i} L_f^{\rho_i - 1} h_i(x)$ of the scalar functions $h_i(x)$, $i = 1, \dots, m$, are computed as shown in [25] and [24]. Note that the control law (2) is well defined in the domain $D \subset \mathbb{R}^n$ if the *decoupling matrix* $J(x)$ is non-singular at every point $x_0 \in D \subset \mathbb{R}^n$. The new input vector $v(t)$ can be designed with any linear control technique. The relative degree of the whole system (1) in this case is defined as

$$\rho = \sum_{k=1}^m \rho_k \quad (3)$$

Depending on the value of the relative degree ρ , three following cases are considered. First, if $\rho = n$, then the nonlinear system (1) is fully feedback linearizable. Second, if $\rho < n$, then the nonlinear system (1) is partially feedback linearizable. In this case, there are some internal dynamics of order $(n - \rho)$.

For tracking control, these dynamics must be guaranteed to be internally stable. Third, if ρ does not exist on the domain $D \subset \mathbb{R}^n$, then the input-output linearization technique is not applicable. In this case, a virtual output $\tilde{y}(t) = \tilde{h}(x)$ may be introduced such that the new system becomes feedback linearizable [25]. The linearized system for the two first cases can be represented under the following *normal form* [23]:

$$\begin{cases} \dot{\xi}(t) = A\xi(t) + Bv(t) \\ y(t) = C\xi(t) \\ \dot{\omega}(t) = f_0(z(t), v(t)) \end{cases} \quad (4)$$

with $z(t) \triangleq [\xi(t), \omega(t)]^T$, where $\xi(t) \in \mathbb{R}^\rho$ and $\omega(t) \in \mathbb{R}^{n-\rho}$ are obtained with a suitable change of coordinates $z(t) = T(x(t)) \triangleq [T_1(x(t)), T_2(x(t))]^T$. The triplet (A, B, C) is in Brunovsky block canonical form. The system $\dot{\omega}(t) = f_0(z(t), v(t))$ characterizes the internal dynamics [23]. Note that if this system is input-to-state stable, then the origin of system (4) is globally asymptotically stable [24].

3. LMI-based robust control design

Modeling errors are unavoidable in real-world applications, especially when using PMA approximation [22]. Thus, a robust design is necessary to robustify the feedback linearization control scheme. This section provides a new robust control approach to deal with this major practical issue. For convenience, the feedback linearization control law (2) is rewritten as

$$u(x) = \alpha(x) + \beta(x)v(t) = \alpha(x) - \beta(x)K\xi(t) = \alpha(x) - \beta(x)KT_1(x) \quad (5)$$

where K is the control gain of the new linearizing controller. The terms $\alpha(x)$ and $\beta(x)$ are directly derived from (2). Due to modeling uncertainty, the real implemented feedback control law can be represented in the form

$$u(x) = \tilde{\alpha}(x) - \tilde{\beta}(x)K\tilde{T}_1(x) \quad (6)$$

where $\tilde{\alpha}(x)$, $\tilde{\beta}(x)$, and $\tilde{T}_1(x)$ are, respectively, the approximations of $\alpha(x)$, $\beta(x)$, and $T_1(x)$. Then, the closed-loop system (4) can be rewritten as

$$\begin{cases} \dot{\xi}(t) = (A - BK)\xi(t) + B\Delta(z) \\ \dot{\omega}(t) = f_0(z(t), v(t)) \end{cases} \quad (7)$$

where

$$\Delta(z) = \beta^{-1}(x) \{ \tilde{\alpha}(x) - \alpha(x) + [\beta(x) - \tilde{\beta}(x)]KT_1(x) + \tilde{\beta}(x)K[T_1(x) - \tilde{T}_1(x)] \} \Big|_{x=T^{-1}(z)} \quad (8)$$

The uncertain term $\Delta(z)$ is viewed as a perturbation of the nominal system $\dot{\xi}(t) = (A - BK)\xi(t)$. Assume that the internal dynamics is input-to-state stable. Then, the stability of the system

$$\dot{\xi}(t) = (A - BK)\xi(t) + B\Delta(z) \quad (9)$$

with respect to the uncertain term $\Delta(z)$ is studied. To this end, we assume that the uncertain term $\Delta(z)$ satisfies the following quadratic inequality [29]:

$$\Delta^T(z)\Delta(z) \leq \delta^2 \xi^T(t) H^T H \xi(t) \Big|_{z=[\xi, \omega]} \quad (10)$$

where $\delta > 0$ is a bounding parameter and the matrix $H \in \mathbb{R}^{l \times \rho}$, characterizing the system uncertainties [19], is constant for a certain integer l . Inequality (10) can be rewritten as

$$\begin{bmatrix} \xi(t) \\ \Delta(z) \end{bmatrix}^T \begin{bmatrix} -\delta^2 H^T H & 0 \\ 0 & I \end{bmatrix} \begin{bmatrix} \xi(t) \\ \Delta(z) \end{bmatrix} \leq 0 \quad (11)$$

where I denotes identity matrix of appropriate dimension.

Consider the Lyapunov function candidate $V(\xi(t)) = \xi^T(t) P \xi(t)$, where $P \in \mathbb{R}^{\rho \times \rho}$, $P = P^T > 0$. The time derivative of $V(\xi)$ along the trajectory of (9) is given by

$$\dot{V}(\xi(t)) = \xi^T(t) \left((A - BK)^T P + P(A - BK) \right) \xi(t) + \Delta^T(z) P \xi(t) + \xi^T(t) P \Delta(z) \quad (12)$$

If $\dot{V}(\xi(t))$ is negative definite, then this system is robustly stable. This condition is equivalent to

$$\begin{bmatrix} \xi(t) \\ \Delta(z) \end{bmatrix}^T \begin{bmatrix} (A - BK)^T P + P(A - BK) & P \\ P & 0 \end{bmatrix} \begin{bmatrix} \xi(t) \\ \Delta(z) \end{bmatrix} < 0 \quad (13)$$

for all $\xi(t)$ and $\Delta(z)$ satisfying (11). By the S-procedure [28], condition (13) holds if and only if there exists a scalar $\tau > 0$ such that

$$\begin{bmatrix} (A - BK)^T P + P(A - BK) + \tau \delta^2 H^T H & P \\ P & -\tau I \end{bmatrix} < 0 \quad (14)$$

Pre- and post-multiplying (14) with the matrix $\text{diag}[\tau P^{-1}, I]$ and then using the change of variable $Y = \tau P^{-1} > 0$, condition (14) is equivalent to

$$\begin{bmatrix} (A - BK)Y + Y(A - BK)^T + \delta^2 YH^T H Y & I \\ I & -I \end{bmatrix} < 0 \quad (15)$$

By Schur complement lemma [28], the condition (15) is equivalent to

$$\begin{bmatrix} (A - BK)Y + Y(A - BK)^T & I & YH^T \\ I & -I & 0 \\ HY & 0 & -\gamma I \end{bmatrix} < 0 \quad (16)$$

where $\gamma \triangleq 1/\delta^2$. Using the change of variable $L \triangleq KY$, the control design can be formulated as an LMI problem in Y , L , and γ as follows:

$$\begin{bmatrix} AY + YA^T - BL - L^T B^T & I & YH^T \\ I & -I & 0 \\ HY & 0 & -\gamma I \end{bmatrix} < 0 \quad (17)$$

To prevent the unacceptably large control feedback gains for practical applications, the amplitude of the entries of K should be constrained in the optimization problem. To this end, the following LMIs can be included:

$$\begin{bmatrix} -\kappa_L I & L^T \\ L & -I \end{bmatrix} < 0, \quad \kappa_L > 0$$

$$\begin{bmatrix} Y & I \\ I & \kappa_Y I \end{bmatrix} > 0, \quad \kappa_Y > 0.$$
(18)

Note that condition (18) implies $K^T K < \kappa_L \kappa_Y^2 I$ (see [29]). Moreover, to guarantee some prescribed robustness bound $\bar{\delta}$, the following LMI conditions can be also included:

$$\gamma - 1/\bar{\delta}^2 < 0$$
(19)

The above development can be summarized in the following.

Theorem 1. Given a positive scalar $\bar{\delta}$. If there exist matrices $Y > 0$, L , positive scalars γ , κ_L , κ_Y such that the following LMI optimization problem is feasible:

$$\text{minimize } \lambda_1 \gamma + \lambda_2 \kappa_L + \lambda_3 \kappa_Y$$
(20)

subject to LMI conditions (17)–(19).

Then, the closed-loop system (9) is robustly stable, and the state feedback control law is defined as $u(t) = -K\xi(t)$ where $K \triangleq LY^{-1}$.

The weighting factors λ_1 , λ_2 , and λ_3 are chosen according to the desired trade-off between the guaranteed robustness bound $\bar{\delta}$ and the size of the stabilizing gain matrix K . The LMI optimization problem can be effectively solved with numerical toolboxes (e.g., [30, 31]).

4. Application to turbocharged SI air system control

The turbocharged air system of a SI engine is illustrated in **Figure 1**. The nomenclature related to the studied system is shown in **Table 1**.

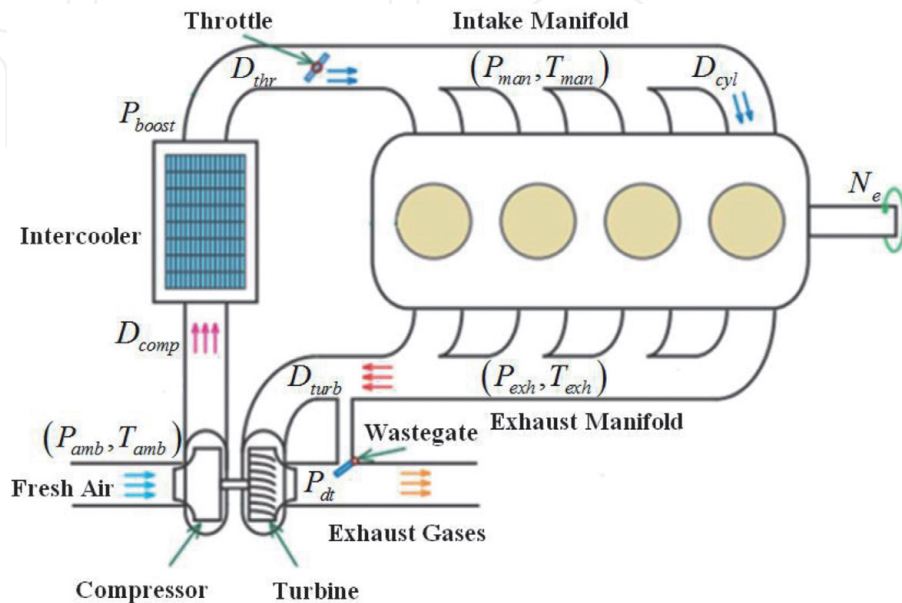


Figure 1.
Schematic of a turbocharged spark-ignition engine.

Symbol	Quantity	Unit	Symbol	Quantity	Unit
Π_{thr}	Throttle pressure ratio	—	D_{cyl}	Cylinder mass airflow	kg/s
Π_{wg}	Wastegate pressure ratio	—	D_{fuel}	Fuel injected flow	kg/s
Π_{comp}	Compressor pressure ratio	—	V_{exh}	Exhaust manifold volume	m ³
Π_{turb}	Turbine pressure ratio	—	V_{man}	Intake manifold volume	m ³
P_{boost}	Boost pressure	Pa	V_{cyl}	Cylinder volume	m ³
P_{man}	Intake pressure	Pa	N_e	Engine speed	rpm
P_{exh}	Exhaust pressure	Pa	\mathbb{P}_{comp}	Compressor power	W
P_{dt}	Turbine pressure	Pa	N_{tc}	Turbocharger speed	rpm
P_{amb}	Atmospheric pressure	Pa	\mathbb{P}_{turb}	Turbine power	W
T_{amb}	Atmospheric temperature	°K	η_{comp}	Compressor isentropic efficiency	—
T_{man}	Intake manifold temperature	°K	η_{turb}	Turbine isentropic efficiency	—
T_{exh}	Exhaust manifold temperature	°K	η_{vol}	Engine volumetric efficiency	—
D_{thr}	Throttle mass airflow	kg/s	λ_s	Stoichiometric air/fuel ratio	—
D_{wg}	Wastegate mass airflow	kg/s	γ	Ratio of specific heats	—
D_{comp}	Compressor mass airflow	kg/s	R	Ideal gas constant	J/kg/°K
D_{turb}	Turbine mass airflow	kg/s	C_p	Specific heats at constant pressure	J/kg/°K

Table 1.
 Notations of turbocharged air system of a SI engine.

4.1 Description of turbocharged air system

Hereafter, a brief description of the air system of a turbocharged SI engine is recalled (see [17, 20, 32] for more details). The model was built with the real data of a four-cylinder turbocharged SI engine from Renault Company (see [19] and [18] for more details). The system dynamics is composed of the three following main parts. First, the intake pressure dynamics is given by

$$\frac{dP_{man}}{dt} = -\eta_{vol} \frac{V_{cyl}}{V_{man}} \frac{N_e}{30} P_{man} + \frac{P_{boost} \sqrt{RT_{man}}}{V_{man}} \Phi_{thr}(\Pi_{thr}^*) u_{thr} \quad (21)$$

where $\Phi(\Pi_{thr}^*) = \sqrt{\frac{2\gamma}{\gamma-1} \left(\Pi_{thr}^{*\frac{2}{\gamma}} - \Pi_{thr}^{*\frac{\gamma+1}{\gamma}} \right)}$ with $\Pi_{thr}^* \triangleq \max \left(\frac{P_{man}}{P_{boost}}, \left(\frac{2}{\gamma+1} \right)^{\frac{\gamma}{\gamma-1}} \right)$ and the volumetric efficiency $\eta_{vol} \triangleq \text{LUT}_{\eta_{vol}}(N_e, P_{man})$ is given by LUT. Second, the exhaust pressure dynamics is expressed as follows:

$$\frac{dP_{exh}}{dt} = \frac{RT_{exh}}{V_{exh}} \left(\left(1 + \frac{1}{\lambda_s} \right) \eta_{vol} \frac{P_{man} V_{cyl} N_e}{RT_{man} 30} - D_{turb} - \Phi_{wg}(\Pi_{wg}^*) \frac{P_{exh}}{\sqrt{RT_{exh}}} u_{wg} \right) \quad (22)$$

where $\Phi(\Pi_{wg}^*) = \sqrt{\frac{2\gamma}{\gamma-1} \left(\Pi_{wg}^{*\frac{2}{\gamma}} - \Pi_{wg}^{*\frac{\gamma+1}{\gamma}} \right)}$ with $\Pi_{wg}^* \triangleq \max \left(\frac{P_{dt}}{P_{exh}}, \left(\frac{2}{\gamma+1} \right)^{\frac{\gamma}{\gamma-1}} \right)$ and the gas flow through the turbine $D_{turb} \triangleq \text{LUT}_{D_{turb}} \left(N_{tc}, \frac{P_{dt}}{P_{exh}} \right)$ is given by LUT. Another turbine gas flow model based on the standard equation for compressible flow across an orifice is also available in [33]. Third, the dynamics of the turbocharger can be modeled as

$$\frac{d}{dt} \left(\frac{1}{2} J_{tc} N_{tc}^2 \right) = \mathbb{P}_{turb} - \mathbb{P}_{comp} \quad (23)$$

where the powers of the turbine and the compressor are given by

$$\begin{cases} \mathbb{P}_{turb} = D_{turb} C_p T_{exh} \eta_{turb} \left(1 - \Pi_{turb}^{\frac{1-\gamma}{\gamma}} \right) \\ \mathbb{P}_{comp} = D_{comp} C_p T_{amb} \frac{1}{\eta_{comp}} \left(\Pi_{comp}^{\frac{\gamma-1}{\gamma}} - 1 \right) \end{cases} \quad (24)$$

In expression (24), the following quantities are given by LUTs

$$\eta_{turb} \triangleq \text{LUT}_{\eta_{turb}} \left(N_{tc}, \frac{P_{dt}}{P_{exh}} \right), \Pi_{comp} \triangleq \text{LUT}_{\Pi_{comp}} \left(N_{tc}, D_{comp} \right), \text{ and } \eta_{comp} \triangleq \text{LUT}_{\eta_{comp}} \left(N_{tc}, \frac{P_{boost}}{P_{amb}} \right).$$

From (23) and (24), the turbocharger dynamics can be rewritten as follows:

$$\frac{d}{dt} \left(\frac{1}{2} J_{tc} N_{tc}^2 \right) = D_{turb} C_p T_{exh} \eta_{turb} \left(1 - \Pi_{turb}^{\frac{1-\gamma}{\gamma}} \right) - D_{comp} C_p T_{amb} \frac{1}{\eta_{comp}} \left(\Pi_{comp}^{\frac{\gamma-1}{\gamma}} - 1 \right) \quad (25)$$

From (21), (22), and (25), the dynamical model of turbocharged air system is given as

$$\begin{cases} \frac{dP_{man}}{dt} = -\eta_{vol} \frac{V_{cyl}}{V_{man}} \frac{N_e}{30} P_{man} + \frac{P_{boost} \sqrt{RT_{man}}}{V_{man}} \Phi_{thr}(\Pi_{thr}^*) u_{thr} \\ \frac{dP_{exh}}{dt} = \frac{RT_{exh}}{V_{exh}} \left(\left(1 + \frac{1}{\lambda_s} \right) \eta_{vol} \frac{P_{man} V_{cyl} N_e}{RT_{man} 30} - D_{turb} - \Phi_{wg}(\Pi_{wg}^*) \frac{P_{exh}}{\sqrt{RT_{exh}}} u_{wg} \right) \\ \frac{d}{dt} \left(\frac{1}{2} J_{tc} N_{tc}^2 \right) = D_{turb} C_p T_{exh} \eta_{turb} \left(1 - \Pi_{turb}^{\frac{1-\gamma}{\gamma}} \right) - D_{comp} C_p T_{amb} \frac{1}{\eta_{comp}} \left(\Pi_{comp}^{\frac{\gamma-1}{\gamma}} - 1 \right) \end{cases} \quad (26)$$

The following features of the turbocharged engine model, directly related to the proposed control solution, should be highlighted [32].

1. This system is highly nonlinear and apparently complex for control design.
2. There are two control inputs (throttle and wastegate) and only one output of interest, the intake pressure, which is directly related to the engine torque.
3. The relation between the wastegate and the intake pressure is not direct.
4. Note that the most commonly available sensors on series production vehicles are found in the intake side of the engine, i.e., the pressure and temperature in the upstream of the compressor (P_{amb}, T_{amb}), the boost pressure P_{boost} , the mass airflow through the compressor D_{comp} , the intake pressure and temperature (P_{man}, T_{man}), and the engine speed N_e .

4.2 MIMO control design

Most of the existing controllers in the open literature, not only aforementioned available measures of engine intake side but also several other signals coming from the exhaust side, i.e., P_{exh}, T_{exh}, P_{dt} , and N_{tc} , are needed for control implementation.

However, these signals are not measured in commercial vehicles and usually assumed to be estimated by estimators/observers. To avoid this practical issue, here these variables are approximated by their static LUTs issued from the data measured in steady-state conditions in the test bench. Hence, we can reduce the number of costly vehicle sensors or/and complex observers. Concretely, the following LUTs are constructed:

$$\begin{cases} P_{exh} = \text{LUT}_{P_{exh}}(N_e, P_{man}) \\ T_{exh} = \text{LUT}_{T_{exh}}(N_e, D_{cyl}) \\ P_{dt} = \text{LUT}_{P_{dt}}(N_e, D_{cyl}) \\ N_{tc} = \text{LUT}_{N_{tc}}(\Pi_{comp}, D_{comp}) \end{cases} \quad (27)$$

Remark from (27) that all the inputs of respective LUTs P_{exh} , T_{exh} , P_{dt} , N_{tc} can be obtained with available vehicle sensors. The approximations in (27) are reasonable since SI engines operate at stoichiometric conditions, which implies that all exhaust variables are highly correlated to the in-cylinder air mass flow (or intake pressure). Note also that although such an approximation may introduce some estimation errors, especially during the transient phases, the proposed robust control approach is expected to compensate these errors.

We now focus on the robust control design. Apart from the output of interest $y_{man} = P_{man}$, we virtually introduce the second output $y_{exh} = P_{exh}$ to facilitate the control design task. Note that the goal is only to track the intake pressure reference $P_{man,ref}$. Moreover, we do not have the exhaust pressure reference $P_{exh,ref}$ in practice. However, by means of LUT in (27), we can impose that $P_{exh,ref} = \text{LUT}_{P_{exh}}(N_e, P_{man,ref})$ and then if P_{exh} converges to $P_{exh,ref}$, it implicitly makes P_{man} converge to $P_{man,ref}$. Hence, both outputs P_{man} and P_{exh} are used to track the intake pressure reference. For engine control design, we consider the two pressure dynamics in (21) and (22), which can be rewritten in the following compact form:

$$\begin{cases} \dot{P}_{man} = K_{man}(D_{thr} - D_{cyl}) \triangleq f_{thr} + g_{thr}u_{thr} \\ \dot{P}_{exh} = K_{exh}(K_{fuel}D_{cyl} - D_{turb} - D_{wg}) \triangleq f_{wg} + g_{wg}u_{wg} \\ y_{man} \triangleq P_{man}, \quad y_{exh} \triangleq P_{exh} \end{cases} \quad (28)$$

where

$$\begin{cases} K_{man} = \frac{RT_{man}}{V_{man}}, \quad K_{exh} = \frac{RT_{exh}}{V_{exh}}, \quad K_{fuel} = \left(1 + \frac{1}{\lambda_s}\right) \\ D_{cyl} = K_{cyl}P_{man}, \quad K_{cyl} = \eta_{vol} \frac{V_{cyl}}{V_{man}} \frac{N_e}{30} \\ f_{thr} = -K_{man}D_{cyl}, \quad f_{wg} = K_{exh}(K_{fuel}D_{cyl} - D_{turb}) \\ g_{thr} = K_{man} \frac{P_{boost}}{\sqrt{RT_{man}}} \Phi_{thr}(\Pi_{thr}^*), \quad g_{wg} = -K_{exh} \frac{P_{exh}}{\sqrt{RT_{exh}}} \Phi_{wg}(\Pi_{wg}^*) \end{cases} \quad (29)$$

Now, the feedback linearization technique is applied to control the nonlinear system (28). To this end, let us compute the time derivatives of the outputs as

$$\begin{cases} \dot{y}_{man} = \dot{P}_{man} = f_{thr} + g_{thr}u_{thr} = v_{man} \\ \dot{y}_{exh} = \dot{P}_{exh} = f_{wg} + g_{wg}u_{wg} = v_{exh} \end{cases} \quad (30)$$

The two control inputs u_{thr} , u_{wg} appear respectively in \dot{y}_{man} , \dot{y}_{exh} ; the signals v_{man} and v_{exh} are two new manipulated inputs. Using an integral structure for tracking control purposes, the following linearized system is derived from (28):

$$\begin{cases} \dot{y}_{man} = v_{man} \\ \dot{y}_{exh} = v_{exh} \\ \dot{x}_{int} = y_{man,ref} - y_{man} \end{cases} \quad (31)$$

with the feedback linearization control laws

$$\begin{cases} u_{thr} = -\frac{f_{thr}}{g_{thr}} + \frac{1}{g_{thr}} v_{man} \\ u_{wg} = -\frac{f_{wg}}{g_{wg}} + \frac{1}{g_{wg}} v_{exh} \end{cases} \quad (32)$$

Define $x \triangleq [y_{man}, y_{exh}, x_{int}]^T$, $v \triangleq [v_{man}, v_{exh}]^T$, and suppose that system (28) is subject to modeling errors $\Delta(x)$ caused by nonlinearities f_{thr} , g_{thr} , f_{wg} , g_{wg} and the approximation by using LUTs. Then, the linearized system (31) is rewritten as

$$\dot{x} = \begin{pmatrix} 0 & 0 & 0 \\ 0 & 0 & 0 \\ -1 & 0 & 0 \end{pmatrix} x + \begin{pmatrix} 1 & 0 \\ 0 & 1 \\ 0 & 0 \end{pmatrix} v + \begin{pmatrix} 0 \\ 0 \\ 1 \end{pmatrix} y_{man,ref} + \Delta(x) \quad (33)$$

We assume that $\Delta(x) \leq \delta^2 x^T H^T H x$. Theorem 1 can be applied to design v_{man} and v_{exh} . Selecting $H = I$, $\lambda_1 = 1$, $\lambda_2 = \lambda_3 = 0$, and $\bar{\delta} = 0.9$, then we obtain the following control law:

$$v = -Kx = -\begin{bmatrix} 110.3 & 0 & -4052 \\ 0 & 48.9 & 0 \end{bmatrix} x \quad (34)$$

and $\delta = 0.9983$, which is larger than prescribed value of $\bar{\delta}$, as expected.

The stability analysis of the internal dynamics is necessary to make sure that the state N_{tc}^2 is well behaved. To this end, the turbocharger dynamics (25) is rewritten in the form

$$\frac{d}{dt}(N_{tc}^2) = K_{turb} D_{turb} - K_{comp} D_{comp} \quad (35)$$

where

$$K_{turb} \triangleq \frac{2}{J_{tc}} C_p T_{exh} \eta_{turb} \left(1 - \Pi_{turb}^{\frac{1-\gamma}{\gamma}}\right); \quad K_{comp} \triangleq \frac{2}{J_{tc}} C_p T_{amb} \frac{1}{\eta_{comp}} \left(\Pi_{comp}^{\frac{\gamma-1}{\gamma}} - 1\right) \quad (36)$$

Moreover, we obtain from (28) and (30) that

$$D_{turb} = K_{fuel} D_{cyl} - D_{wg} - \frac{v_{exh}}{K_{exh}} \quad (37)$$

It follows from (35) and (37) that

$$\frac{d}{dt}(N_{tc}^2) = -K_{turb} D_{wg} - K_{comp} D_{comp} + K_{turb} K_{fuel} D_{cyl} - \frac{K_{turb}}{K_{exh}} v_{exh} \quad (38)$$

Note that $P \triangleq [P_{man}, P_{exh}]^T$ can be considered as the input vector of system (38). Then, it follows that

$$\begin{aligned} \frac{d}{dt}(N_{tc}^2) &< \left(K_{turb}K_{fuel}K_{cyl}P_{man} + \frac{K_{turb}}{K_{exh}}K_{(2,2)}P_{exh} \right) - K_{comp}D_{comp} \\ &\leq \sqrt{(K_{turb}K_{fuel}K_{cyl})^2 + \left(\frac{K_{turb}}{K_{exh}}K_{(2,2)}\right)^2} \|P\| - K_{comp}D_{comp} \triangleq \alpha(t)\|P\| - \beta(N_{tc}^2) \end{aligned} \quad (39)$$

Since α is bounded and the function $\beta(\cdot)$ is of class \mathcal{K}^∞ (see **Figure 2**). Hence, we can conclude that system (35) is input-to-state stable [34].

Hereafter, the controller designed in this subsection is called *conventional MIMO controller*.

4.3 Fuel-optimal control strategy

We have designed in this work *conventional MIMO controller* with two inputs, throttle and wastegate, and two outputs: intake pressure and exhaust pressure for the whole engine operating zone. From the viewpoint of energy efficiency, this controller is not *optimal* in the sense of energy losses minimization. Indeed, the wastegate should be opened as much as possible at a given operating point to minimize the pumping losses [15]. This leads to the control strategy proposed in [16], i.e., in low-load zone, only the throttle is used to track the intake pressure and the wastegate is widely open, and in high-load zone, the wastegate is solely activated to control the pressure and the throttle is widely open in this case. To fully take into account the above fuel-optimal strategy, we propose the so-called fuel-optimal controller for turbocharged air system of a SI engine. This novel controller is directly derived from *conventional MIMO controller*, and they both have the same control law (34). The idea is presented in the sequel.

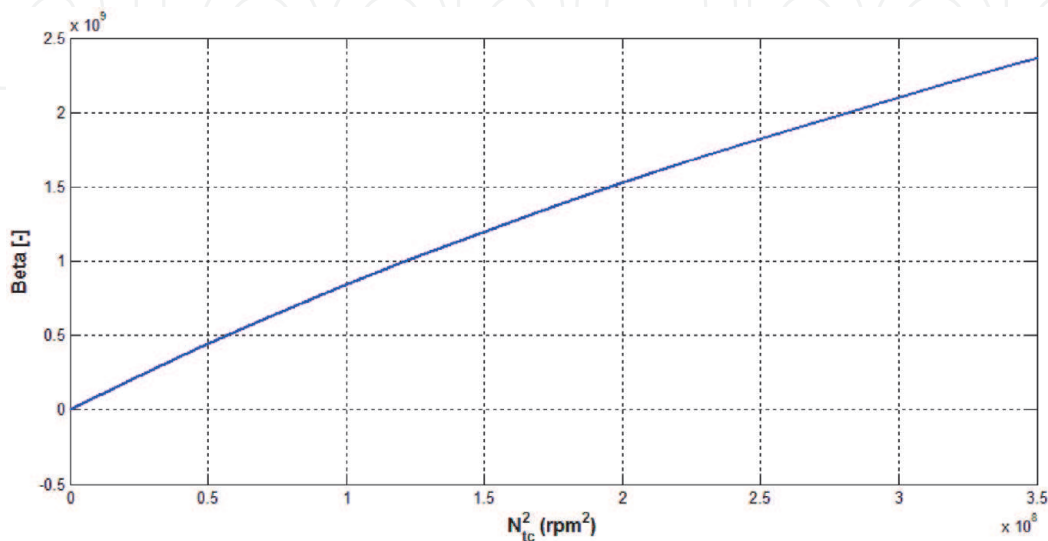


Figure 2.
 Behavior of $\beta(N_{tc}^2)$ function.

Let us recall the engine model (28) as

$$\begin{cases} \dot{P}_{man} = K_{man}(D_{thr} - D_{cyl}) \triangleq f_{thr} + g_{thr}u_{thr} = v_{man} \\ \dot{P}_{exh} = K_{exh}(K_{fuel}D_{cyl} - D_{turb} - D_{wg}) \triangleq f_{wg} + g_{wg}u_{wg} = v_{exh} \\ y_{man} \triangleq P_{man} \\ y_{exh} \triangleq P_{exh} \end{cases} \quad (40)$$

It follows from the second equation of (40) that

$$D_{cyl} = \frac{v_{exh}}{K_{exh}K_{fuel}} + \frac{D_{turb}}{K_{fuel}} + \frac{D_{wg}}{K_{fuel}} \quad (41)$$

Then, the intake pressure dynamics can be also rewritten as

$$\dot{P}_{man} = K_{man} \left(D_{thr} - \frac{v_{exh}}{K_{exh}K_{fuel}} - \frac{D_{turb}}{K_{fuel}} - \frac{D_{wg}}{K_{fuel}} \right) \quad (42)$$

or equivalently

$$\dot{P}_{man} = g_{thr}u_{thr} - \frac{K_{man}}{K_{exh}K_{fuel}}v_{exh} - \frac{K_{man}}{K_{fuel}}D_{turb} + \frac{K_{man}}{K_{exh}K_{fuel}}g_{wg}u_{wg} = v_{man} \quad (43)$$

The novel *fuel-optimal controller* is directly derived from the above expression. To this end, the whole engine operating range is divided into three zones according to two predefined intake pressure thresholds P_{man1} and P_{man2} .

1. *Zone 1* (low-load zone $P_{man} \leq P_{man1}$): The wastegate is widely open, and the throttle is solely used to track the intake pressure reference. Let $S_{wg, \max}$ be the maximal opening section of the wastegate. The implemented actuator control laws are in this case

$$\begin{cases} u_{thr} = \frac{1}{g_{thr}} \left(\frac{K_{man}}{K_{exh}K_{fuel}}v_{exh} + \frac{K_{man}}{K_{fuel}}D_{turb} - \frac{K_{man}}{K_{exh}K_{fuel}}g_{wg}S_{wg, \max} + v_{man} \right) \\ u_{wg} = S_{wg, \max} \end{cases} \quad (44)$$

2. *Zone 2* (middle-load zone $P_{man1} < P_{man} < P_{man2}$): Both throttle and wastegate are simultaneously used to control the intake pressure. In this case, the implemented actuator control laws are exactly the feedback linearization laws in (32), which are recalled here

$$\begin{cases} u_{thr} = -\frac{f_{thr}}{g_{thr}} + \frac{1}{g_{thr}}v_{man} \\ u_{wg} = -\frac{f_{wg}}{g_{wg}} + \frac{1}{g_{wg}}v_{exh} \end{cases} \quad (45)$$

3. *Zone 3* (high-load zone $P_{man} \geq P_{man2}$): The throttle is fully opened, and only the wastegate is activated to control the intake pressure which is approximated by the boost pressure P_{boost} . The implemented actuator control laws are

$$\begin{cases} u_{thr} = S_{thr, \max} \\ u_{wg} = \frac{K_{exh}K_{fuel}}{K_{man}g_{thr}} \left(\frac{K_{man}}{K_{exh}K_{fuel}} v_{exh} + \frac{K_{man}}{K_{fuel}} D_{turb} - g_{thr} S_{thr, \max} + v_{man} \right) \end{cases} \quad (46)$$

where $S_{thr, \max}$ is the maximal opening section of the throttle.

Several remarks can be reported for this actuator scheduling strategy. First, since the input vector $v \triangleq [v_{man}, v_{exh}]^T$ is the same for all three zones, then the dynamics of N_{tc}^2 defined in (35) is always input-to-state stable with this strategy since it does not directly depend on the real control inputs u_{thr} and u_{wg} of the turbocharged air system. Second, the exhaust pressure dynamics can be rewritten as

$$\begin{aligned} \dot{P}_{exh} &= K_{exh}K_{fuel}K_{cyl}P_{man} - K_{exh} \left(\frac{P_{exh}}{\sqrt{RT_{exh}}} \Phi_{wg}(\Pi_{wg}^*) u_{wg} + D_{turb} \right) \\ &< K_{exh}K_{fuel}K_{cyl}P_{man} - K_{exh}D_{turb} \triangleq \theta(P_{man}) - \tau(P_{exh}) \end{aligned} \quad (47)$$

Note that the functions $\theta(\cdot)$ and $\tau(\cdot)$ are of class \mathcal{K}^∞ and then the exhaust pressure dynamics is always input-to-state stable with respect to P_{man} . Third, it follows from the above remarks that if the intake pressure tracking performance is guaranteed, then all other variables of the turbocharged air system (26) will be well behaved within three operating zones. Fourth, the model-based *fuel-optimal controller* is based on a dummy switching strategy because no switching model has been used in this approach. Fifth, the pressure thresholds P_{man1} and P_{man2} separating the three zones are *freely* chosen thanks to the propriety of the above third remark. However, the values of P_{man1} , P_{man2} are usually chosen very close for engine efficiency benefits.

Note that *fuel-optimal controller* is different from other existing approaches in the literature. As the approach proposed in [16], this novel controller is a MIMO nonlinear controller which can guarantee the closed-loop stability of the whole turbocharged air system. However, the novel *fuel-optimal controller* is much simpler, and the middle-load zone (Zone 2) is very easily introduced to improve the torque response at high load while maintaining the maximum possible advantage of *fuel-optimal* concept in [15]. The scheduling strategy of *fuel-optimal controller* has also appeared in [35]. However, the control approach in [35] is based on a decentralized linear scheduling PI controller. In addition, the throttle is only *passively* activated in Zone 2, that is, the throttle control is maintained at a constant value obtained from calibration for each operating point of the engine. Moreover, the authors did not show how to choose the intake pressure thresholds and in particular how this choice will effect on the control design. Compared with the control approach in [36] which is also based on feedback linearization, our controller does not need any model simplification task, e.g., neglecting pressure dynamics with respect to turbocharger dynamics according to singular perturbation theory and approximating the turbocharger square speed as a linear function of intake pressure. Note also that the same simplification procedure is carried out for the approach in [16, 17, 20]. Moreover, in [36], the wastegate and the throttle are separately controlled, and the approach cannot take into account the mid-load zone.

4.4 Simulation results and analysis

Hereafter, a series of trials are performed on an engine simulator designed under commercial AMESim platform [18] to show the effectiveness of the proposed method for both cases: *conventional MIMO controller* and *fuel-optimal controller*.

For the sake of clarity, the two commands (throttle, wastegate) are normalized. Then, the control input constraints become $0 \leq \bar{u}_{thr}, \bar{u}_{wg} \leq 100\%$. When $\bar{u}_{thr} = 100\%$ (respectively, $\bar{u}_{wg} = 0\%$), it means that the throttle (resp. wastegate) is fully open. On the reverse, when $\bar{u}_{thr} = 0\%$ (respectively, $\bar{u}_{wg} = 100\%$), the throttle (resp. wastegate) is fully closed. Before starting, note that the proposed controller is easily tuned with only one parameter, the desired robustness bound $\bar{\delta}$ which is the same for all following simulations. The pressure thresholds are chosen as $P_{man,1} = 0.9$ bar and $P_{man,2} = 1.2$ bar.

4.4.1 Comparison between conventional MIMO control and fuel-optimal control

Figures 3 and 4 represent the intake pressure tracking performance and the corresponding actuator commands for *conventional MIMO controller* and *fuel-optimal controller*, respectively. *Conventional MIMO controller* simultaneously uses both actuators to track the intake pressure, while these actuators are optimally scheduled by the strategy described in SubSection 4.3 with *fuel-optimal controller*. The wastegate is opened very little with *conventional MIMO controller* so that the boost potential of the turbocharger can be fully exploited. Hence, the closed-loop time response with this controller is faster than the one of *fuel-optimal controller* in middle- and high-load zones. Moreover, although *conventional MIMO controller* can be used to improve the torque response (drivability), this controller is not optimal in terms of fuel consumption compared with *fuel-optimal controller* as pointed out in **Figure 5**. The pumping losses with *fuel-optimal controller* are almost lower than the ones with *conventional MIMO controller* at every time. Observe that the pumping losses with *fuel-optimal controller* are very low at high intake pressure.

Since the goal of this work is to design a controller minimizing the energy losses, only results with the *fuel-optimal controller* will be presented in the rest of this chapter.

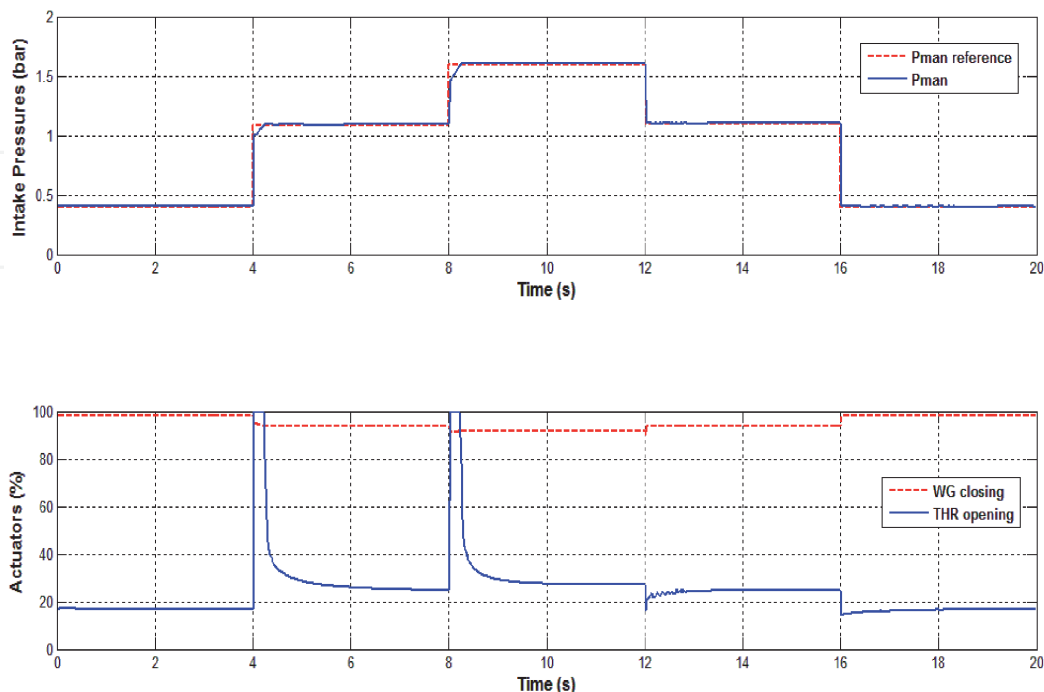


Figure 3. Pressure tracking performance (up) and corresponding actuator commands (bottom) with conventional MIMO controller at $N_e = 2000$ rpm.

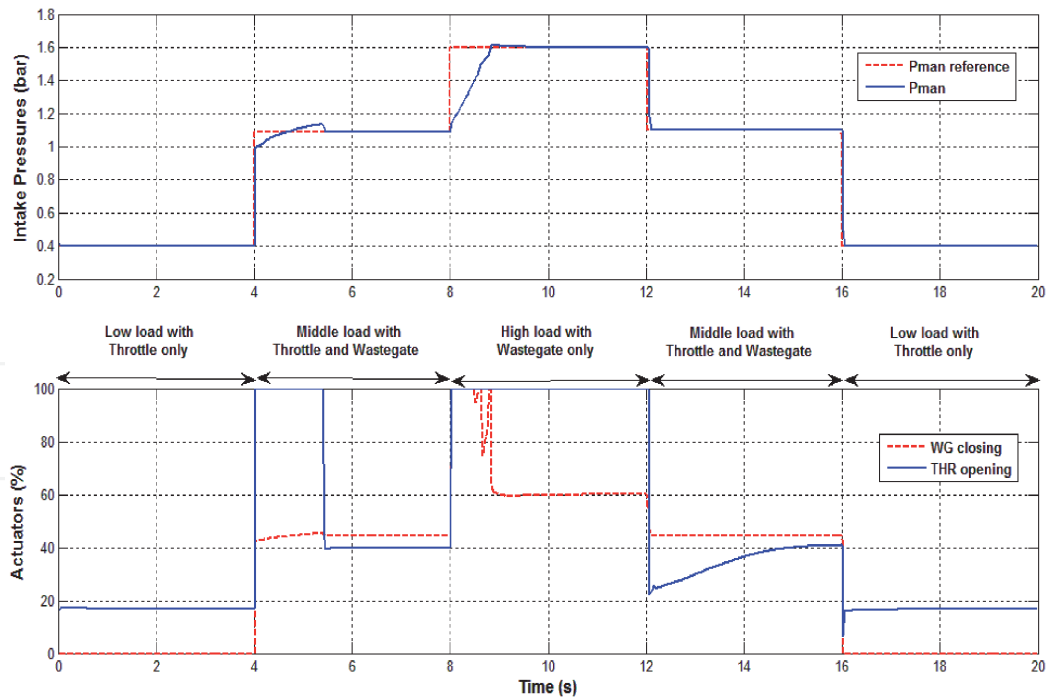


Figure 4. Pressure tracking performance (up) and corresponding actuator commands (bottom) with fuel-optimal controller at $N_e = 2000$ rpm.

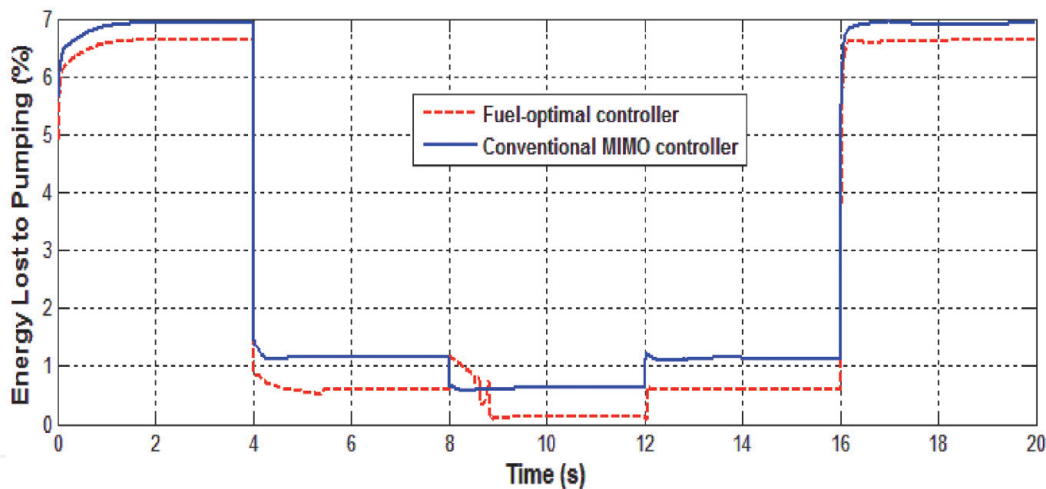


Figure 5. Comparison of engine pumping losses between conventional MIMO controller and fuel-optimal controller at $N_e = 2000$ rpm.

4.4.2 Fuel-optimal controller performance at different engine speeds

The trajectory tracking of the intake pressure at different engine speeds is shown in **Figure 6**. The following comments need to be made regarding these results. First, the tracking performance is very satisfying over the whole operating range. The wastegate command is very aggressive during the turbocharger transients; it hits the constraints and then stabilizes to track the boost pressure. This fact allows compensating the slow dynamics of the turbocharger. Moreover, this behavior can be easily tuned with the parameter $\bar{\delta}$, i.e., a smaller value of $\bar{\delta}$ leads to the faster time response; however the robustness bound will be reduced. Second, the controller does not generate any overshoot in the considered operating range which is also a very important property for the driving comfort.

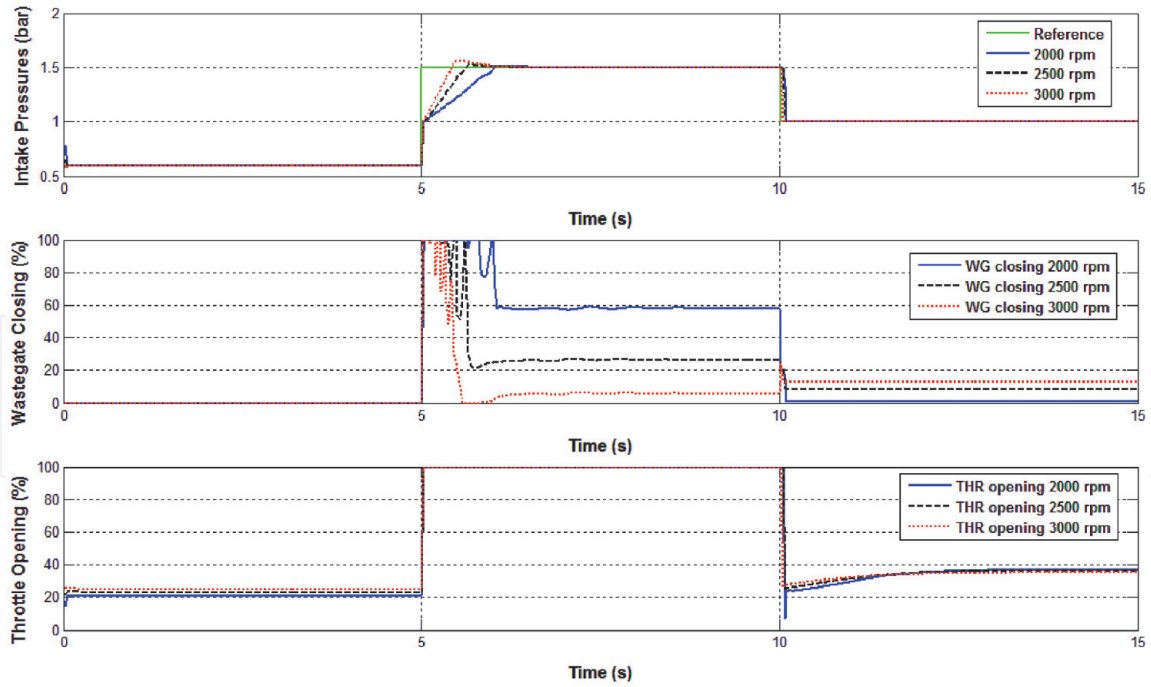


Figure 6. Intake pressure tracking performance (up) with corresponding wastegate commands (middle) and throttle commands (bottom) at different engine speeds.

4.4.3 Vehicle transients

The closed-loop responses during the vehicle transient are presented in **Figure 7**. It can be noticed that the *fuel-optimal controller* is perfectly able to guarantee a very good tracking performance even with the important variation of the engine speed (which represents the vehicle transient).

All of the above test scenarios and the corresponding results confirm the effectiveness of the proposed approach over the whole engine operating range. It is

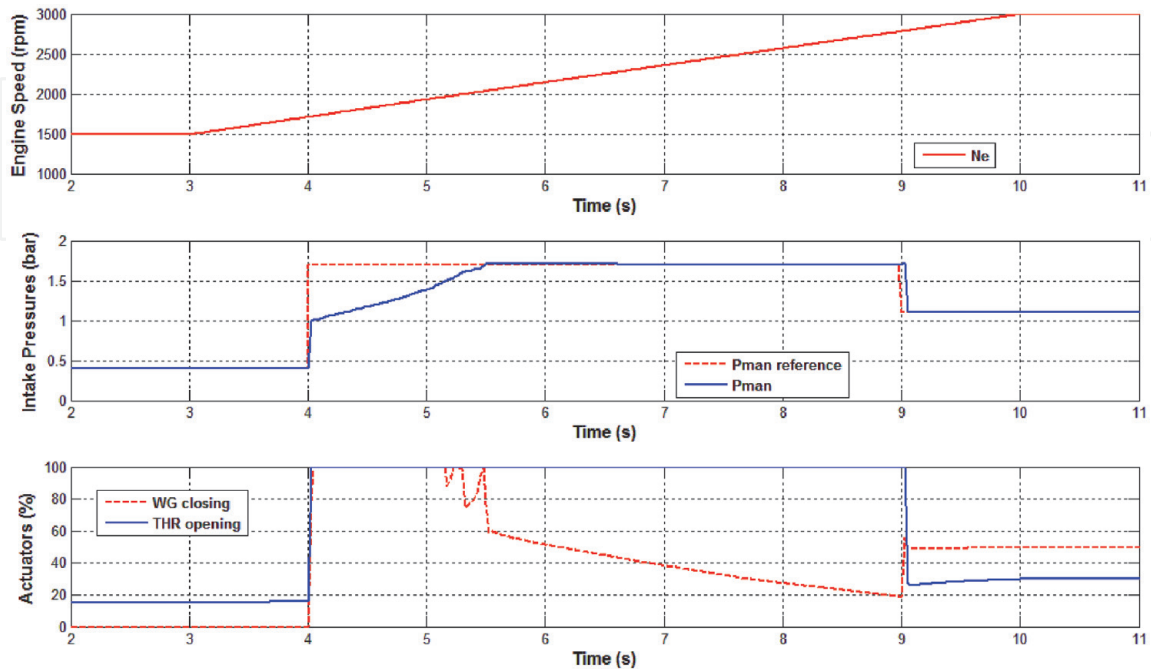


Figure 7. Variation of engine speed (up) and pressure tracking performance (middle) with corresponding actuator commands (bottom) for a vehicle transient.

emphasized again that the same controller gain is used for both controllers in all simulations. Therefore, the proposed approach requires very limited calibration effort.

5. Concluding remarks

A new robust control design has been proposed to handle the modeling uncertainty and/or disturbances, known as one of major drawbacks of feedback linearization. Compared to the existing results, the proposed method provides a simple and constructive design procedure which can be recast as an LMI optimization problem. Hence, the controller feedback gain is effectively computed.

In terms of application, an original idea has been proposed to control the turbocharged air system of a SI engine. Several advantages of this approach can be summarized as follows. First, the second virtual output $y_{exh} \triangleq P_{exh}$ is introduced by means of LUT, and this fact drastically simplifies the control design task. Second, the resulting nonlinear control law is easily implementable. Third, offline engine data of the test bench is effectively reused and exploited for engine control development so that the number of sensors and/or observers/estimators could be significantly reduced. Finally, the controller is robust with respect to modeling uncertainties/disturbances, and its feedback gain can be effectively computed through a convex optimization problem with available numerical solvers. Despite its simplicity, the proposed controller can provide very promising results for both control strategies of turbocharged air system, i.e., to improve the drivability with *conventional MIMO controller* or to optimize the fuel consumption with *fuel-optimal controller*. Future works focus on the real-time validation of the proposed fuel-optimal control strategy with an engine test bench.


IntechOpen

Author details

Anh-Tu Nguyen*, Thierry-Marie Guerra and Jimmy Lauber
Laboratory LAMIH UMR CNRS 8201, Université Polytechnique Hauts-de-France,
Valenciennes, France

*Address all correspondence to: nguyen.trananhtu@gmail.com

IntechOpen

© 2020 The Author(s). Licensee IntechOpen. Distributed under the terms of the Creative Commons Attribution - NonCommercial 4.0 License (<https://creativecommons.org/licenses/by-nc/4.0/>), which permits use, distribution and reproduction for non-commercial purposes, provided the original is properly cited. 

References

- [1] Moulin P. Air systems modeling and control for turbocharged engines [PhD thesis]. MINES Paristech; 2010
- [2] Guzzella L, Onder C. Introduction to Modeling and Control of Internal Combustion Engine Systems. Berlin Heidelberg: Springer-Verlag; 2004
- [3] Daubler L, Bessai C, Predelli O. Tuning strategies for online-adaptive PI controller. Oil and Gas Science and Technology. 2007;**62**(4):493-500
- [4] Karnik A, Buckland J, Freudenberg J. Electronic throttle and wastegate control for turbocharged gasoline engines. American Control Conference. Portland; 2005. pp. 4434-4439
- [5] Jung M, Glover K, Christen U. Comparison of uncertainty parameterisations for H-infinity robust control of turbocharged diesel engines. Control Engineering Practice. 2005; **13**(1):15-25
- [6] Wei X, del Re L. Gain scheduled H_{∞} control for air path systems of diesel engines using LPV techniques. IEEE Transactions on Control Systems Technology. 2007;**15**(3):406-415
- [7] Utkin V, Chang H, Kolmanovsky I, Cook J. Sliding mode control for variable geometry turbocharged diesel engines. In: American Control Conference. Chicago; 2000. pp. 584-588
- [8] Ortner P, del Re L. Predictive control of a diesel engine air path. IEEE Transactions on Control Systems Technology. 2007;**15**(3):449-456
- [9] Kim S, Jin H, Choi S. Exhaust pressure estimation for diesel engines equipped with dual-loop EGR and VGT. IEEE Transactions on Control Systems Technology. 2017;**26**(2):382-392
- [10] Wang H, Bosche J, Tian Y, El Hajjaji A. Two loop based dynamical feedback stabilization control of a diesel engine with EGR & VGT. In: 50th IEEE Conference on Decision and Control and European Control Conference (CDC-ECC). Orlando, USA; 2011. pp. 1596-1601
- [11] Zhang Y, Lu G, Xu H, Li Z. Tuneable model predictive control of a turbocharged diesel engine with dual loop exhaust gas recirculation. Proceedings of the Institution of Mechanical Engineers, Part D. 2018; **232**(8):1105-1120
- [12] Laguech S, Aloui S, El Hajjaji A, Chaari A. Fuzzy sliding mode control for turbocharged diesel engine. Journal of Dynamic Systems, Measurement, and Control. 2016;**138**(1):011009
- [13] Gong X, Wang Y, Chen H, Hu Y. Double Closed-Loop Controller Design for Boost Pressure Control of Turbocharged Gasoline Engines. Vol. 7. IEEE Access; 2019. pp. 97333-97342
- [14] Hu Y, Chen H, Wang P, Chen H, Ren L. Nonlinear model predictive controller design based on learning model for turbocharged gasoline engine of passenger vehicle. Mechanical Systems and Signal Processing. 2018; **109**:74-88
- [15] Eriksson L, Frei S, Onder C, Guzzella L. Control and optimization of turbocharged SI engines. 15th IFAC World Congress. Barcelona, Spain; 2002
- [16] Nguyen A-T, Dambrine M, Lauber J. Lyapunov-based robust control design for a Class of switching nonlinear systems subject to input saturation: Application to engine control. IET Control Theory and Applications. 2014a;**8**(17):1789-1802
- [17] Nguyen A-T, Lauber J, Dambrine M. Robust H_{∞} control design for switching uncertain system: Application for

- turbocharged gasoline air system control. In: 51st Annual Conference on Decision and Control (CDC). Maui, Hawaii, USA: IEEE; 2012a. pp. 4265-4270
- [18] Nguyen A-T, Lauber J, Dambrine M. Optimal control based algorithms for energy management of automotive power systems with battery/supercapacitor storage devices. *Energy Conversion and Management*. 2014b;87:410-420
- [19] Nguyen A-T, Lauber J, Dambrine M. Multiobjective control design for turbocharged spark ignited air system: A switching Takagi-Sugeno model approach. In: American Control Conference (ACC). Washington, DC, USA: IEEE; 2013. pp. 2866-2871
- [20] Nguyen A-T, Lauber J, Dambrine M. Switching fuzzy control of the air system of a turbocharged gasoline engine. In: IEEE International Conference on Fuzzy Systems (FUZZ-IEEE). Brisbane: IEEE; 2012b. pp. 1-7
- [21] Nguyen A-T, Sugeno M, Campos V, Dambrine M. LMI-based stability analysis for piecewise multi-affine systems. *IEEE Transactions on Fuzzy Systems*. 2016;25(3):707-714
- [22] Nguyen A-T, Taniguchi T, Eciolaza L, Campos V, Palhares R, Sugeno M. Fuzzy control systems: Past, present and future. *IEEE Computational Intelligence Magazine*. 2019;14(1):56-68
- [23] Isidori A. *Nonlinear Control Systems*. London: Springer Verlag; 1989
- [24] Khalil H. *Nonlinear Systems*. 3rd ed. Upper Saddle River, NJ: Prentice Hall; 2002
- [25] Sastry S. *Nonlinear Systems*. New York: Springer-Verlag; 1999
- [26] Ha I, Gilbert E. Robust tracking in nonlinear systems. *IEEE Transactions on Automatic Control*. 1987;32(9):763-771
- [27] Kravaris C, Palanki S. A Lyapunov approach for robust nonlinear state feedback synthesis. *IEEE Transactions on Automatic Control*. 1988;33(12):1188-1191
- [28] Boyd S, Ghaoui L, Feron E, Balakrishnan V. *Linear Matrix Inequalities in System and Control Theory*. Philadelphia: Society for Industrial and Applied Mathematics (SIAM); 1994
- [29] Šiljak D, Stipanović D. Robust stabilization of nonlinear systems: The LMI approach. *Mathematical Problems in Engineering*. 2000;6(5):461-493
- [30] Gahinet P, Nemirovski A, Laub A, Chilali M. *LMI Control Toolbox*. Apple Hill Drive: The Math Works Inc.; 1995
- [31] Lofberg J. *YALMIP: A toolbox for modeling and optimization in MATLAB*. In: IEEE International Symposium on Computer Aided Control Systems Design. Taipei; 2004. pp. 284-289
- [32] Nguyen A-T. *Advanced Control Design Tools for Automotive Applications [PhD thesis]*. University of Valenciennes et du Hainaut-Cambresis; 2013
- [33] Eriksson L. Modeling and control of turbocharged SI and DI engines. *Oil and Gas Science and Technology*. 2007; 62(4):523-538
- [34] Sontag E, Wang Y. On characterizations of the input to state stability property. *Systems and Control Letters*. 1995:351-359
- [35] Gorzelic P, Hellström E, Stefanopoulou A, Jiang L, Gopinath S. A coordinated approach for throttle and wastegate control in turbocharged spark ignition engines. 24th Chinese Control and Decision Conference. Taiyuan, China; 2012. pp. 1524-1529
- [36] Moulin P, Chauvin J. Modeling and control of the air system of a turbocharged gasoline engine. *Control Engineering Practice*. 2011;19(3):287-297